AN INTRODUCTION TO METEOSAT SECOND GENERATION (MSG)

BY JOHANNES SCHMETZ, PAOLO PILI, STEPHEN TJEMKES, DIETER JUST, JOCHEN KERKMANN, SERGIO ROTA, AND ALAIN RATIER

Meteosat Second Generation (MSG), the new generation of European geostationary meteorological satellites, has greatly enhanced capabilities, especially for observing rapidly changing weather phenomena and for the derivation of quantitative products.

The meteorological community has benefited for more than two decades from the services of the current generation of the European geostationary meteorological Meteosat satellites, the first of which was launched in 1977. Since then it was followed by six successful launches of Meteosat satellites and *Meteosat-7* is currently the operational satellite at the nominal position at 0° longitude. The Meteosat series will be replaced by a new generation called Meteosat Second Generation (MSG). MSG provides the user community with continuity of services from the current Meteosat system, but will also significantly enhance services and products. As is the current Meteosat series, MSG satellites are spin stabilized (Fig. 1). However, MSG gives significantly increased information due to an imaging-repeat cycle of 15 min

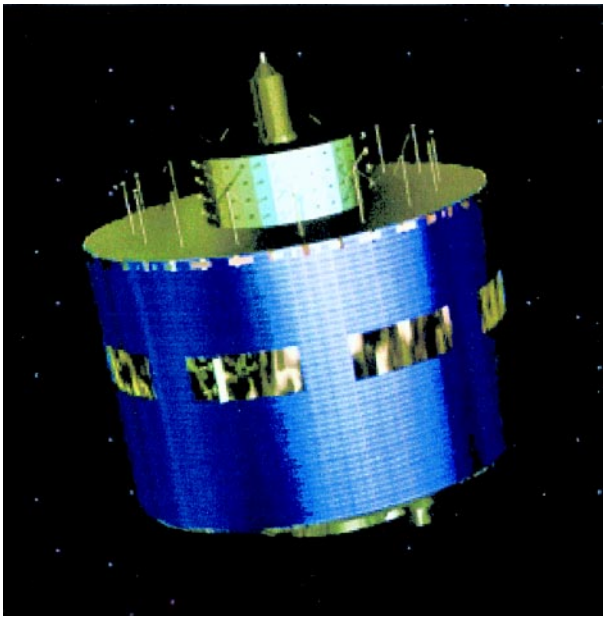

FIG. 1. MSG spacecraft; as with the current Meteosat series, MSG satellites are spin stabilized.

AFFILIATIONS: SCHMETZ, PILI, TJEMKES, JUST, KERKMANN, ROTA, AND RATIER—EUMETSAT, Darmstadt, Germany
Supplements to this article are available online (DOI: 110.1175/BAMS-83-7-Schmetz-1; DOI: 110.1175/BAMS-83-7-Schmetz-2). For current information see:
http://dx.doi.org/110.1175/BAMS-83-7-Schmetz-1 and
http://dx.doi.org/110.1175/BAMS-83-7-Schmetz-2.
CORRESPONDING AUTHOR: Dr. Johannes Schmetz, EUMETSAT, Am Kavalleriesand 31, D-64295 Darmstadt, Germany
E-mail: schmetz@eumetsat.de

In final form 14 May 2002

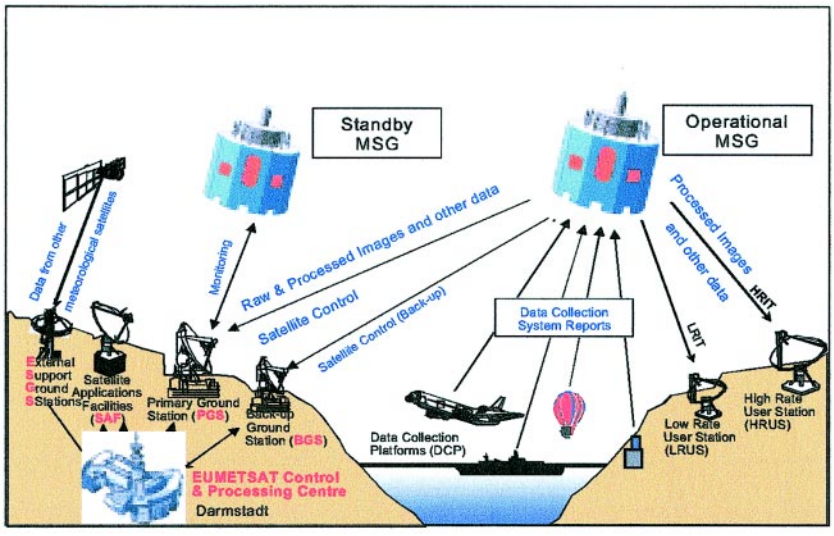

Fig. 2. MSG system and mission concept illustrating the two-satellite service whereby one satellite is in stand-by mode.

(30 min for Meteosat) and 12 spectral channels (3 channels for Meteosat), quantization with 10 bits per pixel (8 for Meteosat), and image sampling distances of 3 km at nadir for all channels except the high-resolution visible with 1 km (for Meteosat, 5 and 2.5 km, respectively). The advent of MSG is the most significant upgrade of the meteorological observing capabilities in geostationary orbit since the launch of the GOES-I (renamed *GOES-8;* see the appendix for a list of acronyms) in 1994 (Menzel and Purdom 1994). *GOES-8* and the subsequent GOES satellites carry a 5-channel imager and an 18-channel infrared sounder. Other geostationary meteorological satellites are operated by China, India, Japan, and Russia, and nowadays, they are an indispensable part of the global observing system. They are the key source for timely information on rapid weather development, and the monitoring of tropical storms and large midlatitude systems.

The MSG program covers a series of three identical satellites, MSG-1, -2, and -3 (at the time of this paper these satellites had not been launched), which are expected to provide observations and services over at least 12 yr. Each satellite has an expected lifetime of 7 yr. MSG-1 is scheduled for launch in 2002 with MSG-2 to follow nominally 18 months later, thus providing a standby satellite in orbit. The MSG system is established under a cooperation between the European Space Agency (ESA) and the European Organisation for the Exploitation of Meteorological Satellites (EUMETSAT). A European consortium, led by the Rutherford Appleton Laboratory (RAL) in the United Kingdom (UK), provides an additional research instrument, the Geostationary Earth Radiation Budget (GERB) instrument, for flights on all three

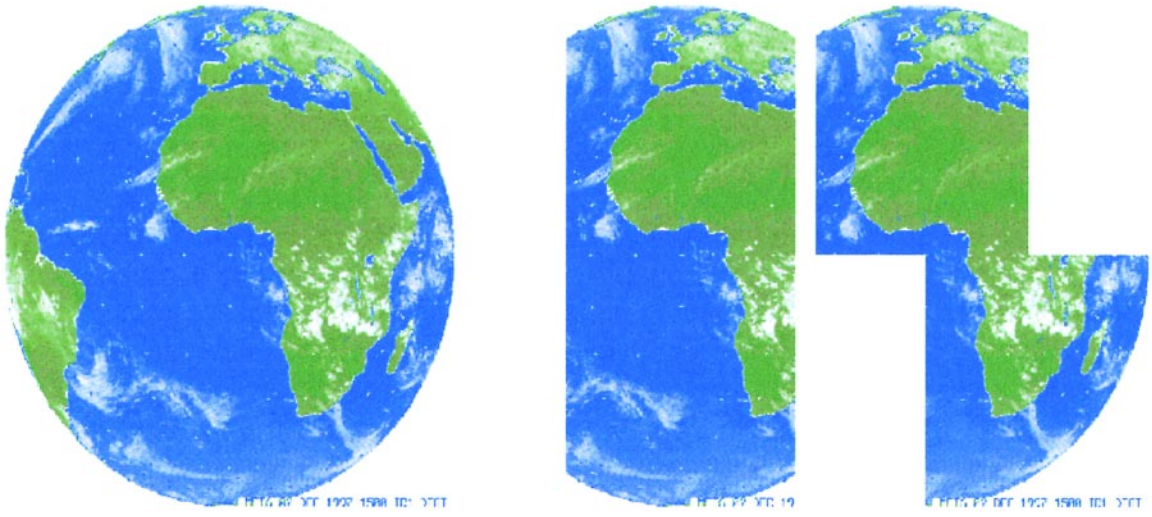

Fig. 3. Coverage with SEVIRI on MSG, in its nominal position at 0° lon, for a repeat cycle of 15 min for channels 1–11 (see Table 1). The full disk image has 3712 × 3712 pixels. The HRV (right-hand side of figure) covers only half of the earth in the E–W direction with 11 136 × 5568 pixels; however, the area of imaging can be selected. Scanning of SEVIRI is from east to west and south to north.

MSG satellites and also the associated data services. ESA is responsible for the development of the MSG-1 prototype satellite according to EUMETSAT requirements and also acts as procurement agent for the MSG-2/3 satellites. EUMETSAT formulates and maintains end user requirements, procures all launch services, develops the ground segment, ensures overall system consistency, and operates the MSG system over a nominal period of 12 yr. MSG is planned as a two-satellite operational service, like the current Meteosat system, where one satellite is available in orbit as a spare (see Fig. 2).

This paper introduces MSG with emphasis on its capabilities, products, and applications. Section 2 describes the main instrument SEVIRI, section 3 summarizes the ground segment, and section 4 describes products including future developments. Sections 5 and 6 are short summaries of the data access and the radiation budget instrument (GERB), respectively. The appendix provides a list of acronyms used in this paper. Technical details on the radiometric performance of SEVIRI, its calibration, and its image characteristics are described in the sidebar and online (http://dx.doi.org/10.1175/BAMS-83-7-Schmetz-1 and http://dx.doi.org/10.1175/BAMS-83-7-Schmetz-2).

SEVIRI INSTRUMENT. The primary mission of MSG is the continuous observation of the earth's full disk. This is achieved with the Spinning Enhanced Visible and Infrared Imager (SEVIRI) imaging radiometer. SEVIRI is a 12-channel imager observing the earth–atmosphere system. Eleven channels observe the earth's full disk with a 15-min repeat cycle. A high-resolution visible (HRV) channel covers half of the full disk in the east–west direction and a full disk in the north–south direction (see Fig. 3). The high-resolution visible channel has a spatial resolution of 1.67 km, as the oversampling factor is 1.67 the sampling distance is 1 km at nadir. The corresponding values for the eight thermal IR and the other three solar channels are 4.8-km spatial resolution, with an oversampling factor of 1.6 that corresponds to a sampling distance of 3 km for nadir view. The instantaneous field of view (IFOV) corresponds to the area of sensitivity for each picture element. Since the aperture angle for each IFOV is constant, it follows that the corresponding area at the surface varies with satellite-viewing angle. The telescope optical layout is based on a three-mirror concept with a primary mirror of 51 cm in diameter. The focal plane with the IR detectors is passively cooled enabling two controlled temperatures of either 85 or 95 K (see online supplement). The optical bench of the solar channels is at a temperature of 293 K. Instrument mass is 260 kg and power consumption 150 W.

Operating SEVIRI. A repeat cycle of 15 min for full-disk imaging provides unprecedented multispectral observations of rapidly changing phenomena (e.g., deep convection) and provides better and more numerous wind observations from the tracking of rap-

SPATIAL RESOLUTION AND IMAGE GEOMETRIC QUALITY

SEVIRI observes the earth–atmosphere system with a spatial sampling distance of 3 km at subsatellite point in 11 channels. A high-resolution visible (HRV) channel covers half of the full disk with a 1-km spatial sampling at subsatellite point. The actual field of view of the channels is about 4.8 and 1.67 km, respectively, at the subsatellite point. One should note, however, that the detectors are diamond shaped; that is, the 4.8 and 1.67 km views are oriented at an angle of 45° with respect to the E–W and N–S directions. The (detector only) point-spread function in the east–west and north–south is a triangle with a base width of 6.8 km at the subsatellite point for all channels, except the HRV channel. The image acquisition is based on a constant angular stepping, that is, the subtended angle for each pixel remains constant; hence, the spatial resolution of a pixel at the surface decreases with increasing off-nadir viewing angle.

Since most of the quantitative image analyses require multispectral image data, a careful spatial coregistration of channels is needed. Level-1.5 image data from SEVIRI will have interchannel registration of 0.75 km or better for all infrared channels, and for the four solar channels it will be 0.6 km at the subsatellite point. The registration of HRV and non-HRV pixels is done in such a way that the HRV pixel lies at the center of the pixel of the other channels. The absolute accuracy of pixel locations is better than 3 km at subsatellite. Within blocks of 16 × 16 pixels the relative accuracy is better than 0.75 km.

An important application of geostationary observations is the animation of images or temporal image analyses; the tracking of features, such as clouds or water vapor structures, in successive images being a prominent example. This application necessitates an accurate image-to-image relative-accuracy requirement, which is met with an rms value of 1.2 km.

Table 1. Spectral channel characteristics of SEVIRI providing central, minimum, and maximum wavelength of the channels and whether the channel is an absorption or a window channel. A concise summary of the use of the spectral channels is given in the section titled "SEVERI spectral channels."

Channel no.		Characteristics of spectral band (μm)			Main gaseous absorber or window
		λ_{cen}	λ_{min}	λ_{max}	
1	VIS0.6	0.635	0.56	0.71	Window
2	VIS0.8	0.81	0.74	0.88	Window
3	NIR1.6	1.64	1.50	1.78	Window
4	IR3.9	3.90	3.48	4.36	Window
5	WV6.2	6.25	5.35	7.15	Water vapor
6	WV7.3	7.35	6.85	7.85	Water vapor
7	IR8.7	8.70	8.30	9.10	Window
8	IR9.7	9.66	9.38	9.94	Ozone
9	IR10.8	10.80	9.80	11.80	Window
10	IR12.0	12.00	11.00	13.00	Window
11	IR13.4	13.40	12.40	14.40	Carbon dioxide
12	HRV	Broadband (about 0.4 – 1.1)			Window/water vapor

idly changing cloud features. The imaging is performed, by combining satellite spin and rotation (stepping) of the scan mirror. The images are taken from south to north and east to west. The E–W scan is achieved through the rotation of the satellite with a nominal spin rate of 100 revolutions min^{-1}. The spin axis is nominally parallel to the north–south axis of the earth. The scan from south to north is achieved through a scan mirror covering the earth's disk with about 1250 scan lines; this provides 3750 image lines for channels 1–11 (see Table 1) since three detectors for each channel are used for the imaging. For the HRV (channel 12) nine detectors sweep the earth for one line scan. A complete image, that is, the full disk of the earth, consists of nominally 3712 × 3712 pixels for channels 1–11 (see Table 1). The HRV channel covers only half the full disk in the E–W direction (see Fig. 3) and therefore a complete image consists of 11 136 × 5568 pixels. A nominal repeat cycle is a full-disk imaging of about 12 min, followed by the calibration of thermal IR channels with an onboard blackbody that is inserted into the optical path of the instrument. Then the scan mirror returns to its initial scanning position. Within 15 min SEVIRI generates a total of about 2.4 Gbits. It should be noted that the number of line scans is programmable such that shorter repeat cycles (rapid scans) can be performed. The operational utilization of this "rapid scan" capability will be defined with the operational user community once relevant experience has been gained with MSG-1.

SEVIRI Spectral Channels. Most SEVIRI spectral channels (see Table 1) build upon the heritage from other satellites, which has the great advantage that the operational user community can readily use existing know-how to utilize SEVIRI radiance observations. Figure 4 shows the weighting functions of the thermal IR channels at 3.9, 6.2, 7.3, 8.7, 9.7, 10.8, 12.0, and 13.4 μm The weighting functions demonstrate that the channels have been selected such that they provide good information on clouds and the earth's surface, water vapor, and ozone. A combination of channels provides useful information on atmospheric instability. The heritage of the MSG channels can be summarized as follows:

- VIS0.6 and VIS0.8: Known from the Advanced Very High Resolution Radiometer (AVHRR) of the polar-orbiting NOAA satellites. They are essential for cloud detection, cloud tracking, scene identification, aerosol, and land surface and vegetation monitoring.
- NIR1.6: Discriminates between snow and cloud, ice and water clouds, and provides aerosol information. Observations are, among others, available from the Along Track Scanning Radiometer (ATSR) on the Earth Remote Sensing Satellite (ERS).
- IR3.9: Known from AVHRR. Primarily for low cloud and fog detection (Eyre et al. 1984; Lee et al. 1997). Also supports measurement of land and sea surface temperature at night and increases the low-level wind coverage from cloud tracking (Velden et al. 2001). For MSG, the spectral band has been

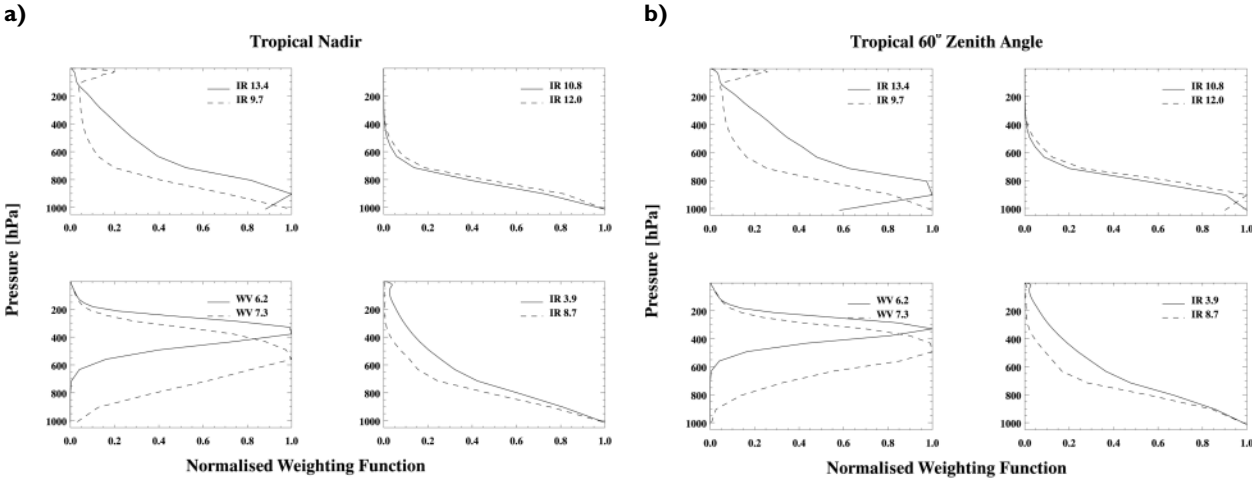

FIG. 4. Weighting functions for the thermal IR channels of SEVIRI on MSG-1. The leftmost four panels in (a) correspond to a tropical standard atmosphere and nadir view; the rightmost four panels in (b) are for a viewing angle of 60°.

broadened to longer wavelengths to improve signal-to-noise ratio.

- WV6.2 and WV7.3: Continues mission of Meteosat broadband water vapor channel for observing water vapor and winds. Enhanced to two channels peaking at different levels in the troposphere (see Fig. 4). Also supports height allocation of semitransparent clouds (Nieman et al. 1993; Schmetz et al. 1993).
- IR8.7: Known from the High Resolution Infrared Sounder (HIRS) instrument on the polar-orbiting NOAA satellites. The channel provides quantitative information on thin cirrus clouds and supports the discrimination between ice and water clouds.
- IR9.7: Known from HIRS and current GOES satellites. Ozone radiances could be used as an input to numerical weather prediction (NWP). As an experimental channel, it will be used for tracking ozone patterns that should be representative for wind motion in the lower stratosphere. The evolution of the total ozone field with time can also be monitored.
- IR10.8 and IR12.0: Well-known split window channels (e.g., AVHRR). Essential for measuring sea and land surface and cloud-top temperatures; also for the detection of cirrus cloud (e.g., Inoue 1987) and volcanic ash clouds (Prata 1989).
- IR13.4: The CO_2 absorption channel known from the former GOES VISSR Atmospheric Sounder (VAS) instrument, where VISSR stands for Visible Infrared Spin-Scan Radiometer. It improves height allocation of tenuous cirrus clouds (Menzel et al. 1983). In cloud-free areas, it will contribute to temperature information from the lower troposphere that can be used for estimating static in-

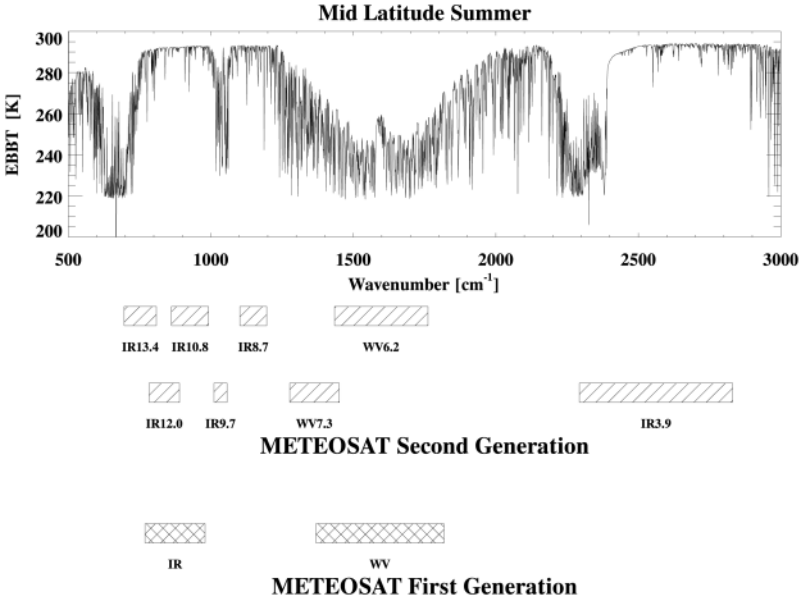

FIG. 5. Thermal infrared part of the spectrum emitted by the earth–atmosphere is shown in the top panel. Brightness temperatures are plotted as a function wavenumber. MSG imager channels are indicated below, as are the channels of the current Meteosat generation.

stability (see GII product in the section titled "Central facilities").

A synopsis of the MSG thermal infrared channels and the channels of the current Meteosat is shown in Fig. 5.

MSG GROUND SEGMENT. The EUMETSAT multimission ground segment comprises a set of (i) central facilities, located at EUMETSAT headquarters, in Darmstadt, Germany; (ii) a primary and a backup ground station for satellite control and data acquisition; and (iii) a geographically distributed network of so-called Satellite Application Facilities (SAFs).

Central facilities. The central facilities control the EUMETSAT satellites through the relevant ground stations and preprocess all data acquired from these satellites up to level 1.5. In the case of MSG, preprocessing is performed by the Image Processing Facility (IMPF), where so-called level-1.5 image data are produced from the level-1 data. The essential processing steps comprise (i) correction for differences in detector response (three detectors for all channels, except the high-resolution visible with nine detectors); (ii) compensation for nonlinearity in a manner similar to the one performed for GOES (Menzel and Purdom 1994); and (iii) geometrical correction into a standard reference projection that also includes the registration between channels. The resulting level-1.5 data have a 10-bit digitization and provide the basis for all further processing and for the derivation of meteorological products. Relevant calibration information is part of the level-1.5 image data stream that is broadcast via the satellite. Operating two MSG satellites in parallel will be possible; for instance, one could operate one MSG satellite in the nominal "full-disk" mode and a second one in rapid scan mode.

Figure 6 depicts key elements of the Applications Ground Segment that extracts meteorological or geophysical (level 2) products from level-1.5 data. It comprises the central Meteorological Product Extraction Facility (MPEF) and a network of seven geographically distributed SAFs. In addition, it features a multimission Unified-Meteorological Archiving and Retrieval Facility (U-MARF) where all data and products, generated centrally, will be archived. The archiving of SAF products will be performed by the SAFs themselves, although an archiving in the U-MARF is considered as well.

Satellite Application Facilities (SAFs). The SAFs are a distributed element of the EUMETSAT applications ground segment. The novel idea behind the network of SAFs is that more products from MSG (and the future EUMETSAT Polar System) can be derived capitalizing on specialized scientific expertise at national meteorological services and other national entities across the member states in Europe. Each SAF is expected to provide operational services to end users, that is, real-time and/or offline product services, distribution of user software packages, and data management. The SAFs also provide the related user services, including the conduct and management of relevant research and development.

Seven SAFs are currently under development, covering seven "themes" agreed to by the EUMETSAT Council. The themes address operational meteorology and other disciplines, which is in line with the new EUMETSAT Convention that extends its charter to climate monitoring. It is clear that the relevance of SAFs to MSG, or vice versa, varies considerably from SAF to SAF. The following briefly summarizes the currently established SAFs and their goals:

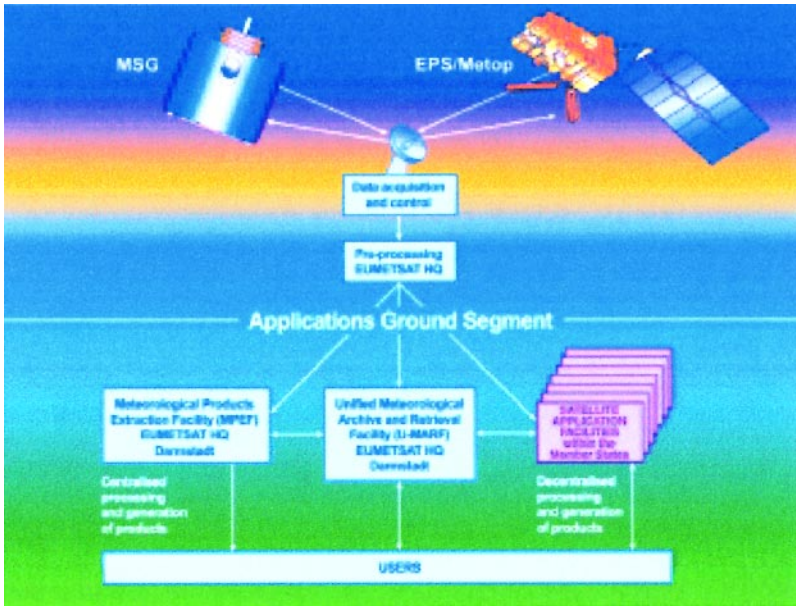

FIG. 6. Overall architecture of the EUMETSAT multimission ground segment. The sketch also includes the future EUMETSAT Polar System (EPS/Metop) planned for launch in 2005.

1) The SAF on "Support to Nowcasting and Very Short Range Forecasting" was established to utilize the new data from MSG and the future EUMETSAT Polar System (EPS) for enhanced nowcasting. Software packages are being developed for the operational extraction of products relevant to nowcasting and will be finally distributed for local installation.
2) The SAF on "Ocean and Sea Ice" will routinely produce and disseminate products characterizing the ocean surface and the energy fluxes across the sea surface.
3) The SAF on "Ozone Monitoring" is being developed for the processing of data on ozone, other trace gases, aerosols, and ultraviolet radiation estimated from satellite observations. Emphasis is on the preparation for the Global Ozone Monitoring Experiment (GOME-2) on EPS.
4) The SAF on "Climate Monitoring" will generate and archive high-quality datasets for specific climate application areas. Currently it concentrates on cloud parameters, radiation budget parameters, and atmospheric humidity composite products.
5) The SAF on "NWP" aims at increasing the benefits to the various European meteorological centers from NWP by developing advanced techniques for the effective use of satellite data.
6) One SAF is dedicated to radio occultation measurements from satellite. It will focus on the Global Positioning System (GPS) Receiver for Atmospheric Sounding (GRAS) instrument to be flown on the EPS planned for launch in 2005. The SAF on "GRAS Meteorology" will provide near-real-time and offline sounding data (temperature, humidity, and pressure) and corresponding validation products as well as software for the assimilation of GRAS data in NWP models.
7) The broad scope of the SAF on "Land Surface Analysis" is to increase the benefit from MSG and EPS data related to land, land–atmosphere interactions, and biospheric applications by developing techniques that will allow a more effective use of satellite data.

MSG PRODUCTS. The derivation of level-2.0 meteorological products in support of NWP, nowcasting, and climatological studies is performed within the applications ground segment (AGS). As outlined above, the AGS consists of (i) a MPEF and (ii) a network of SAFs located at various national weather services and other institutions of EUMETSAT member states. In the following, the MPEF products are briefly introduced and higher-level information on the large number of SAF products is given.

MPEF products. The scene analysis of MSG images is the first step and an intermediate product of the MSG MPEF. The scene analysis algorithm (SCE) is based on multispectral threshold techniques (e.g., Saunders and Kriebel 1988) and classifies all pixels into certain classes. It provides the basis for cloud products and is used in the derivation of other products requiring either cloudy or clear pixels. Scene analyses are supported by radiative transfer model calculations (Tjemkes and Schmetz 1997) helping the interpretation of image data. The radiative transfer calculations use short-term forecast profiles of temperature and humidity from the European Centre for Medium-Range Weather Forecasts (ECMWF) as model input. The results of the scene analysis provide the following as an intermediate product per pixel and per repeat cycle: (i) identification of cloudy and clear pixels and a cloud mask, (ii) identification of scene type, and (iii) radiances at the top of the atmosphere. The cloud mask is available to users through the archive (U-MARF). Advantage is taken of the 15-min repeat cycle by using results of the previous image as a first guess in the current image. SCE and cloud analysis are described in more detail by Lutz (1999).

- *Cloud analysis (CLA)* is based on the scene analysis results and provides, on a scale of 100 km × 100 km (or better), information on cloud cover, cloud-top temperature, cloud-top pressure–height, cloud type, and cloud phase. An important objective of the cloud analysis product is to support the generation of the atmospheric motion vectors (AMV). Therefore an intermediate product for each pixel and repeat cycle, which provides the necessary internal input to the atmospheric motion vectors, is derived, but not disseminated. This intermediate (pixel scale) cloud analysis is also used for the cloud-top height product. It also provides input to the statistical information contained in the offline climate datasets (CDS) product.
- *Cloud-top height (CTH)* is a derived product image, which provides the height of the highest cloud at a superpixel resolution of 3 × 3 pixels. This product is for use in aviation meteorology. It provides the heights with a vertical resolution of 300 m. Additionally the CTH product provides information about fog in the CTH processing segment.
- *Clear-sky radiance (CSR)* gives mean radiances [in W m^{-2} sr^{-1} $(cm^{-1})^{-1}$] for cloud-free pixels (see Fig. 7). Operational NWP centers will use CSR

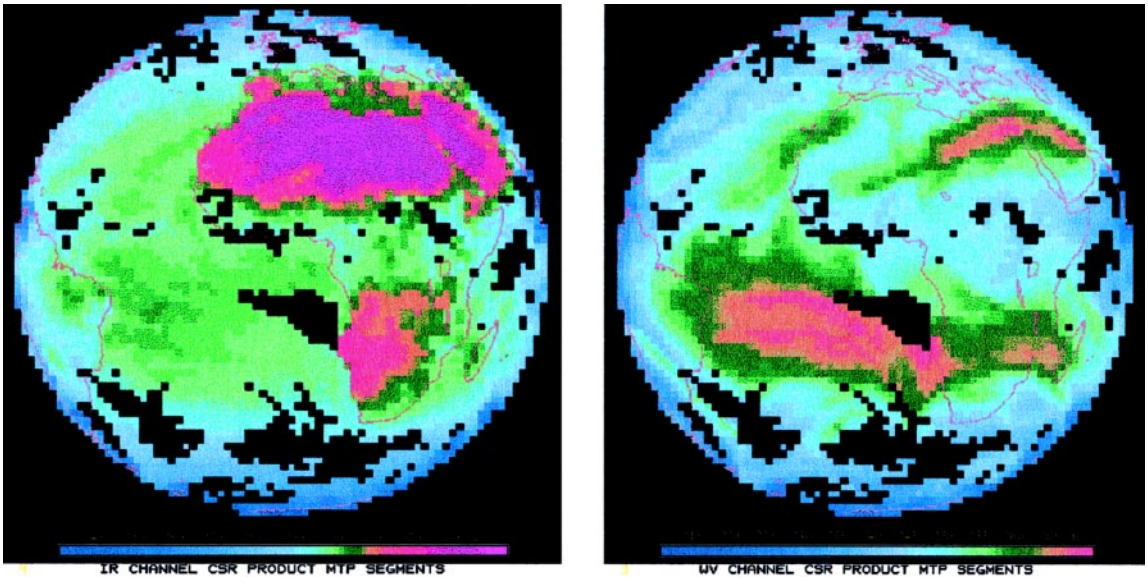

FIG. 7. Clear-sky IR window radiance (left) and (right) clear-sky water vapor (WV) radiance products. Results are from the MSG prototype algorithm applied to *Meteosat*-7 data, where IR and WV channels have a spectral range of 10.5–12.5 and 5.7–7.3 μm, respectively.

products from the MSG infrared channels in their analyses. The benefit will emerge with the advent of 4D variational data assimilation systems that have the capability to utilize the frequent time observations from geostationary orbit (e.g., Munro et al. 1998).

- *Tropospheric humidity (TH)* provides estimates of layer-mean relative humidity for two tropospheric layers. One-layer humidity (between about 500 and 200 hPa) is based on 6.3-μm clear-sky radiances; this product is also known as the upper-tropospheric humidity (UTH) from the current Meteosat MPEF. The mean relative humidity of a second layer (between 850 and 300 hPa) uses clear-sky 7.3-μm radiances and is named midtropospheric humidity (MTH). The algorithm follows the improved UTH retrieval presented in Schmetz et al. (1995), which uses the retrieval from brightness temperature developed by Soden and Bretherton (1993).
- *Atmospheric motion vectors (AMV)* constitute the most important product for numerical weather prediction. The tropospheric AMVs will be derived from cloud and water vapor motion using primarily the 0.6- or 0.8-μm channel, the 10.8-μm channel, and the 6.2- and 7.3-μm channels, respectively. The capability to extract lower-stratospheric displacement vectors from ozone will also be exploited in the future. The product is based on conceptually validated ideas and methods (e.g., Schmetz at al. 1993; Holmlund 2000). An important feature, already implemented in the current Meteosat products, is the improved automatic quality control using quality indicators (Holmlund 1998). The MSG algorithm features new concepts that are improvements over the current Meteosat operational algorithm. These concepts are (i) a wind vector assignment to the exact target position, (ii) improved target selection and enhancement, (iii) improved quality control that benefits from the fact that wind fields from a single repeat cycle are used to derive a spatially dense final AMV product, and (iv) improved height assignment for semitransparent cloud tracers. AMVs will be extracted with smaller template sizes (e.g., 24×24 or 16×16 pixels) than is done in the current Meteosat wind processing, which will greatly improve the spatial coverage of the product.
- *ISCCP dataset (IDS)* continues the support to the International Satellite Cloud Climatology Program (ISCCP) providing three different data formats (Rossow and Schiffer 1999).
- *High-resolution precipitation index (HPI*) continues the support to the Global Precipitation Climatology Project (GPCP) and provides the frequency of pixels for classes of brightness temperatures (Arkin and Xie 1994). Since it is indicative of convective (tropical) rainfall the product is confined to the latitudes between 40°S and 40°N.
- *Climate dataset (CDS)* provides statistical information about the scene classes in a processed segment

(nominally 32 × 32 pixels). It is a concise summary of the radiances observed in a segment and potentially very useful for climatological studies of cloud and radiation fields. Radiation budget studies can usefully employ the CDS (e.g., Schmetz et al. 1990).

- *Global instability index (GII)* is an airmass parameter indicating the stability of the clear atmosphere. For the product retrieval, a scale of about 30 km is foreseen. The GII is related to products from the SAF for nowcasting and very short range forecasting, except that the GII is derived globally and disseminated to users, while the nowcasting SAF provides a software package to derive the instability locally from MSG image data. The idea for the GII emerged from the successful applications and experience by NOAA/NESDIS with GOES lifted index products (Menzel et al. 1998). In addition to the lifted index, the GII product includes information on total precipitable water and other instability indices (König et al. 2001). Six SEVIRI channels at 6.2, 7.3, 8.7, 10.8, 12.0, and 13.4 μm, respectively, are used in the retrieval. It is foreseen that the GII product will be derived with an artificial neural network, which will be trained with results from a physical retrieval (König et al. 2001), and which is based on the work of Ma et al. (1999). The direct implementation of the physical retrieval method for GII retrievals for the full disk is currently not possible due to high computational needs and therefore a neural network will be used. Figure 8 shows an example for the lifted index as calculated with the prototype physical retrieval algorithm for a dataset from the *GOES-8* sounder. The retrieval algorithm uses the GOES sounder channels at 6.2, 6.5, 7.3, 10.8, 12.0, and 13.4 μm; that is, the 6.5-μm channel is used instead of the SEVIRI 8.7-μm channel. Figure 8 (top) shows the lifted index for 4 June 2001 at 1500 UTC; areas of high instability appear red, yellow areas are less unstable. Clouds are shown in gray. Figure 8 (bottom) shows that deep convective clouds have formed in the unstable air over Texas 12 h later.
- *Total ozone product (TOZ)* uses the 9.7-μm channel and other SEVIRI channels and correlative data, and is derived with a regression algorithm (Orsolini and Karcher 2000; Engelen et al. 2001). The ozone observations are useful for monitoring and forecasting UV radiation at the ground level. Preliminary studies have also shown that ozone observations at high temporal and spatial resolution may provide information about the winds in the lower stratosphere (e.g., Riishojgaard 1996). Alternatively, the ozone observations can be assimilated into a dynamical model with a suitable multivariate data assimilation system in which the forecast includes a prognostic equation for ozone.

SAF products. The Satellite Application Facilities have been introduced in section 4. Out of the seven SAFs notably the Ocean and Sea Ice SAF, the Ozone SAF, the Climate SAF, and the Land Surface Analysis SAF

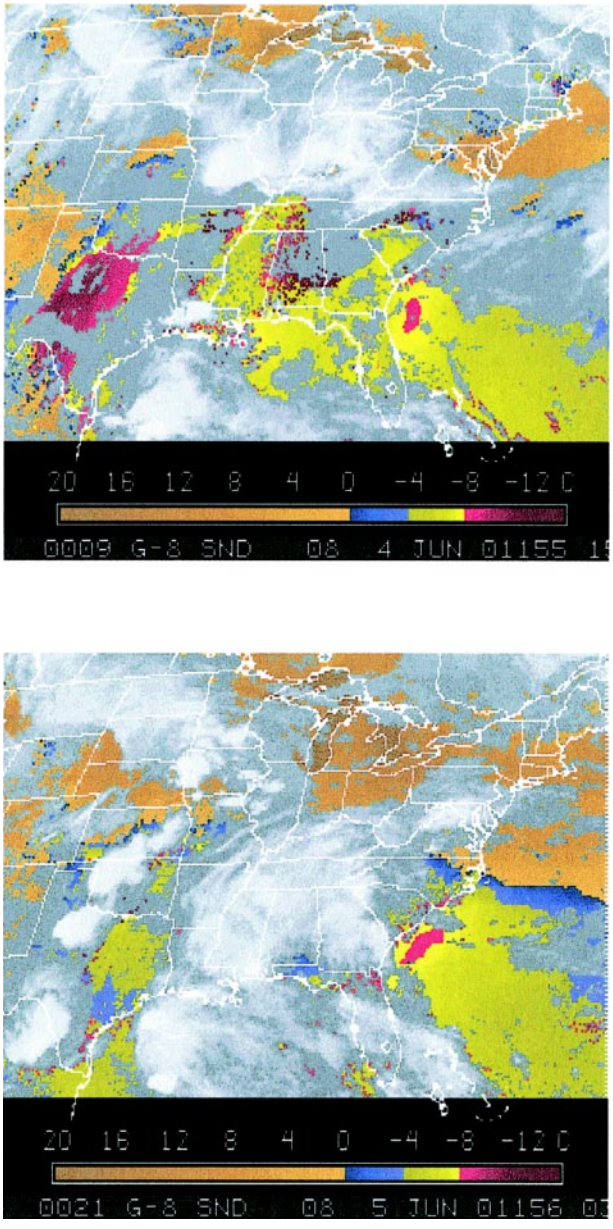

Fig. 8. (top) The lifted index computed with the MSG prototype algorithm (physical retrieval) for *GOES-8* data for 4 Jun 2001 at 1500 UTC. (bottom) The lifted index 12 h later, when deep convective clouds had formed in the unstable area over Texas.

draw on the novel data available from MSG. The list of agreed to and targeted products can be summarized as follows:

- Examples of products from the Ocean and Sea Ice SAF include (i) Atlantic sea surface temperature, (ii) surface radiative fluxes over the Atlantic, (iii) sea ice (polar Atlantic), that is, ice edge/cover/type.
- Examples of products from the Climate SAF are (i) cloud parameters, (ii) surface radiation budget components, (iii) radiation budget components at the top of the atmosphere, and (iv) humidity composite products.
- Examples of targeted products from the Land Surface Analysis SAF are (i) vegetation parameters and biophysical indicators, (ii) snow cover, (iii) land surface temperature, (iv) soil moisture, (v) surface albedo, (vi) evapotranspiration, and (vii) shortwave and longwave radiation parameters.
- The Ozone SAF is responsible for the algorithm development for the total ozone from MSG; however the product derivation is done within the central MPEF.

The above list is exemplary and may undergo further changes. Some products are composites and based on multimission data including MSG data as one source. For more details the interested reader is referred to the relevant SAF Web site (www.eumetsat.de/saf/), which provides more detailed information on SAF products. It is also noted that the SAF in support to nowcasting and very short range forecasting develops software for a suite of products that can be derived from MSG. This software will be made available for local installation.

Development toward improved and new products. The improvement of so-called day-1 products, that is, products available immediately after commissioning, will be a continuous task. Future research and expected feedback on products from users will encourage those developments. Several improvements are already planned. Those are presented in this section along with a broader discussion on the potential of MSG.

Tjemkes and Watts (2000) report on a research study that investigates new ways to perform a scene analysis. The new method uses "optimum estimation" (Rodgers 2000) as a novel way to simultaneously infer a set of cloud parameters and possibly surface features. This new cloud product derives the following cloud properties from SEVIRI observations in a consistent manner: cloud optical thickness, mean particle radius, cloud-top temperature, cloud-top pressure, and cloud phase. The retrieval of the microphysics of cirrus cloud requires especially careful realistic transfer simulations. The sensitivity calculation of Wiegner et al. (1998) indicates the need for high radiometric accuracy for the retrieval of cirrus microphysics. Here the good radiometric performance of SEVIRI (see online supplement) holds promise for success. SEVIRI imagery will also enable the detection of volcanic ash clouds (Watkin et al. 2000).

The particular characteristics of low-level clouds over land (their spatial scale and shorter lifetime) and the complexity of the background (different types of vegetation, temperature gradients, other surface features) make the tracking of these clouds problematic. The utilization of those AMVs in NWP is very limited since NWP centers are not currently assimilating the low-level AMVs over land. In order to improve the quality of low-level winds over land, new target selection, image enhancement, and cloud height and tracking procedures are to be developed. Initial study results are encouraging since they indicate a better depiction of the atmospheric flow and better accuracy (Szantai et al. 2000). Low-level winds over land and ocean will be enhanced by tracking low-level clouds in HRV, 0.6-, 0.8-, and 3.9-μm observations. Ozone motion vectors could be derived from the displacement of total ozone features; however, a direct assimilation of ozone channel radiances in NWP models might be a viable alternative.

MSG will also provide novel perspectives for observing components of the hydrological cycle that undergo rapid changes. Convective cloud processes related to thunderstorms or frontal systems require an appropriate monitoring with a high temporal repeat cycle. In particular, cloud glaciation and precipitation formation occur rapidly and imagery from current geostationary satellites at the 30-min timescale seem to be inadequate for capturing the transient processes that influence precipitation formation. The change with time of the cloud microphysical state, which is observable from multispectral imagery, may provide useful information on the formation of precipitation. Recent work by Rosenfeld and Lensky (1998) shows that the microphysical and precipitation forming processes can be observed with multispectral satellite imagery. Their work also indicates that transformations in the cloud microphysics due to biomass burning smoke and air pollution can be observed. The utility of MSG for the estimation of precipitation has been discussed in detail by Levizzani et al. (2001), who conclude that nowcasting applications will heavily rely upon the multispectral and spatiotemporal features of SEVIRI. Generally speaking the 15-min repeat

cycle of MSG for full-disk imaging is an excellent and unprecedented starting point for the observation of "fast components" of the hydrological cycle (i.e., convection). It matches the typical observation cycle of meteorological weather radars. It remains to be seen whether even more frequent imagery are needed to push the current frontier of our understanding of the life cycle of convective clouds. In principle, MSG provides this possibility if parts of the full disk are imaged with rapid scans at shorter time intervals.

The usefulness of rapid scans from geostationary satellites for the derivation of winds and for nowcasting applications has been demonstrated by various researchers. Hamada (1983) was among the first to suggest intervals of 15 min to better cope with the short lifetime and rapid deformation of cloud targets. Shenk (1991) argued that the optimum time interval for the tracking of cumulus type clouds over land is between 10 min and less than 1 min, whereas displacement of high-level cirrus clouds is fairly well depicted by the standard imaging interval of 30 min. Uchida et al. (1991) studied low-level cloud motion winds around typhoons. They obtained winds of higher spatial density and closer to the typhoon center when using 7.5- and 15-min imaging intervals as opposed to 30-min intervals. Purdom (1996) has also shown that very accurate mesoscale cloud track winds can be determined from rapid scans; primarily he points out the much better target identification. An interesting aspect is also the use of a "cloud or storm relative animation," which helps to identify secondary circulations around cloud systems. Both 1-min and 30-s interval imagery provide the possibility to follow individual clouds even in complex weather situations.

Velden et al. (2000) have studied the optimal time lapse between images for different spectral channels on *GOES-10* for the derivation of winds. Generally speaking the number of winds, and their quality, increases with decreasing time intervals and increasing resolution; specifically they found that (i) the optimum time interval for VIS images with 1-km resolution is 5 min, (ii) for IR window images with 4-km resolution it is 10 min, and (iii) for water vapor images with 8-km resolution it is 30 min. This result indicates the good potential of MSG for the improved derivation of wind fields.

Recently European scientists has also made substantial efforts to utilize the potential of rapid scans; this was largely triggered by requests for rapid scans with *Meteosat-6* in support of the Mesoscale Alpine Programme (MAP) in 1999 (Levizzani et al., 1998). Rosci et al. (2000) use the more frequent image repeat cycle to improve the detection of convective phenomena. Szantai et al. (2000) show that cloud motion winds over land are more numerous when the imaging frequency is reduced from 30 to 15 min. A reduction to 7.5 min provides another, though smaller, gain. Generally it appears that the advantage of rapid scans for the derivation winds from short-lived clouds would justify the scheduling of rapid scans (e.g., Velden et al. 2000). MSG provides unprecedented opportunities in those areas since the nominal full-disk scan is achieved already within 15 min. The potential of shorter scans over limited areas will be investigated once MSG-1 is in orbit.

MSG also provides novel perspectives for applications over land (see Cihlar et al. 1999) because of its multispectral imagery in the visible, near-infrared, and thermal infrared bands. The quantitative application of the visible and near-infrared bands will be facilitated through the development of an accurate operational vicarious calibration (Govaerts et al. 2001). An interesting application is the monitoring of land surface reflectance. The utility of such a product has been demonstrated by Pinty et al. (2000a,b), who derive a Meteosat surface albedo (i.e., confined to the spectral band of the VIS channel of the current generation of Meteosat satellite) with an algorithm accounting for water vapor and ozone absorption, aerosol scattering, and surface anisotropy. The algorithm has been applied to one year, namely 1996, of Meteosat data in order to document the seasonal variations of the surface albedo. The analysis of these results also revealed a potential influence of intense biomass burning activities on seasonal surface albedo changes at the continental scale over Africa (Pinty et al. 2000c). Thus the observations could also contribute to the monitoring of biomass burning. It is expected that the spectral information from MSG will provide a better product since better corrections for aerosol will be possible.

Prins et al. (2001) have studied the use of geostationary satellites, among them MSG, for the monitoring of active fires. They noted that the elevated saturated temperature (> 335 K) in the 3.9-μm band of SEVIRI will minimize the impact of saturation and allow for subpixel fire characterization. The spatial resolution of SEVIRI and the spectral characteristics of the 3.9-μm band does result, however, in a somewhat larger minimum detectable fire size compared to the American GOES and the future Japanese Multifunctional Transport Satellite (MTSAT). Prins et al. (2001) indicate that MSG will be able to detect a fire of about 0.2 hectare (ha) burning at 750 K at the equator and one of 0.5 ha at 50° latitude.

ACCESS TO MSG DATA AND PRODUCTS. MSG image data and derived products can be accessed in real time and in delayed offline mode, that is, from the archive. For real-time access, MSG image data (level 1.5) and selected products can be received with the MSG user stations, using the MSG digital broadcasting/dissemination capabilities. Raw data are received at the ground station (see Fig. 2); processed at the relevant central facility at EUMETSAT in Darmstadt, Germany; and then disseminated again via the satellite. The raw data rate is 3.2 Mb s^{-1}. There are two data streams for the image/data dissemination: (i) the high-rate information transmission (HRIT) with 1 Mb s^{-1}, and (ii) the low-rate information transmission (LRIT) with 128 kb s^{-1}. Both data streams are digital; that is, the current analog service from Meteosat satellites will be replaced by the LRIT.

Correspondingly two types of user stations are planned to be available from the industry, namely, the high-rate user stations (HRUS) and low-rate user stations (LRUS) for the reception of HRIT and LRIT data streams, respectively. To operate a station, a registration is required that will provide the user with a key to receive encrypted data. The stations will acquire the standard format data streams broadcast from the satellite.

The HRIT and LRIT data streams contain level-1.5 data, as well as foreign satellite data, meteorological products, the Meteorological Data Distribution (MDD), and also data from Data Collection Platforms (DCP). The LRIT data stream provides only a subset of the level-1.5 data from SEVIRI; currently the plan is to disseminate 5 out of the 12 SEVIRI channels with a lossy compression in order to reduce data volume. HRIT features a lossless compression algorithm (except for HRV, which is compressed lossy), such that the radiometric accuracy of all image data is fully preserved. Transmitted data are encrypted for both data streams; however, it is important to note that compression and encryption are completely transparent for the EUMETSAT-authorized users; that is, there is no restriction to data access per se. More details on the HRIT/LRIT data streams can be found online at the EUMETSAT Web site. Furthermore, relevant documents can be made available through the EUMETSAT User Service. It is also being considered to develop other means of data access (e.g., via the Internet).

Level 2 products (though not all) generated centrally and by SAFs will also be disseminated in near-real-time to the national meteorological services through the Global Telecommunication System (GTS) of the World Meteorological Organization and the Regional Meteorological Data Communication Network (RMDCN).

All data and products generated at the central facilities in Darmstadt (e.g., by the MPEF) will be available offline through the Unified-Meteorological Archiving and Retrieval Facility (U-MARF; see Fig. 6). SAFs will archive and make available their products in an analogous manner.

GERB. The Geostationary Earth Radiation Budget Experiment (GERB) is a visible-infrared radiometer for earth radiation budget studies (Harries 2000). It makes accurate measurements of the shortwave (SW) and longwave (LW) components of the radiation budget at the top of the atmosphere. It is the first ERB experiment from geostationary orbit. It measures the solar wave band from 0.32 to 4 μm and the total wave band from 0.32 to 30 μm. The LW from 4 to 30 μm is obtained through subtraction. With a nominal pixel size of about 45 × 40 km (N × S × E × W) at nadir view it obtains an absolute accuracy better than 2.4 W m^{-2} sr^{-1} (< 1%) in the SW and better than 0.4 W m^{-2} sr^{-1} for the LW. The channel coregistration with respect to SEVIRI is 3 km at the subsatellite point. The cycle time for full disk is 5 min for both channels (15 min for full radiometric performance). The derivation of products from GERB, that is, radiation budget components at the top of the atmosphere, is described by Dewitte et al. (2000).

The analysis of simultaneous GERB and SEVIRI data provides the basis for novel process studies, for example, on the influence of tropical convection on the regional radiation budget. This may cast new light on the question of the water vapor feedback in tropical regions (e.g., Lindzen et al. 2001).

CONCLUDING REMARKS. The Meteosat Second Generation (MSG) satellites provide a large step forward in our capabilities to observe the earth from geostationary orbit. The earth's full disk is observed with a nominal repeat cycle of only 15 min with 12 spectral channels with a spatial sampling of 3 km. One channel, the high-resolution visible (HRV) channel, even has a sampling distance of only 1 km. Onboard calibration provides an accuracy better than 1 K for thermal IR channels. A vicarious calibration for the solar channels is expected to yield an accuracy of about 5%. Considering the increase of the digitization to 10 bits for all MSG channels as compared to 8 bits for the current Meteosat series, MSG provides about 20 times more information than Meteosat. The high repeat cycle of 15 min enhances

the observation capabilities for rapidly changing phenomena such as cloud and water vapor structures, which helps nowcasting, short-range forecasting, and numerical weather prediction through improved and more frequent products. Recent studies have shown already that more frequent imaging improves the derivation of atmospheric motion vectors (AMVs; e.g., Velden et al. 2000). Thereby the important AMVs will be improved in terms of data coverage and tracking using the different imaging channels. Height assignment of cloudy tracers will be improved with multichannel methods using the IR window channels together with the 13.4-μm channel or the water vapor channels, respectively (Nieman et al. 1993; Menzel et al. 1983). Clear-sky AMVs can be derived at two atmospheric levels using the two water vapor channels at 6.2 and 7.3 μm.

The capabilities of MSG are also expected to be of great value to research in various disciplines. Notably, investigations of convective phenomena should benefit from the operational 15-min observations with spectral channels that allow the retrieval of cloud microphysical parameters and the ambient humidity field. Land applications will benefit from MSG observations by exploiting the fact that the same area can be observed under varying sun illumination conditions throughout a day. The frequent imaging also increases the probability of obtaining a clear-sky radiance from the surface. Pinty et al. (2000b) provided exemplary work on the derivation of a surface albedo climatology from the VIS channel of the current Meteosat series. It is expected that the multispectral MSG observations will provide better performance and that the careful approach toward the vicarious calibration of solar channels fosters new applications.

The new data also present challenges. A major one will be the improved utilization of MSG multispectral image data in weather forecasting (i.e., NWP and nowcasting). Images contain a wealth of information on cloud and humidity structures that can be used to improve the corresponding numerical analyses of humidity and cloud; however, this has only an impact on the very short range forecast if the wind and mass fields are also adjusted in a consistent way. While the sequences of images contain information on dynamical development, this information is mainly used for qualitative applications, such as additional guidance to forecasters. It is important to develop quantitative applications. Future improvements in model spatial resolution, the ability of models to represent humidity and cloud features, together with the development of 4D assimilation systems may provide the basis for the improved utilization of the satellites' image data (Eyre 2001).

Automatic methods for satellite image interpretation in direct support to nowcasting are also developed. Csekits et al. (2000) report on an automatic pattern recognition method that detects convective cells and their progagation. The output of the software provides the forecaster with information on size, temperature, location, development, and displacement of the convective cells.

The meteorological products derived from MSG image data provide continuity for existing products as well as new products and scope for new applications. A novelty, which coincides with the preparation for and the operation of MSG, is the establishment of the network of Satellite Application Facilities (SAFs), which constitute a part of the applications ground segment for MSG. This SAF network provides a broad and structured basis within the user community to utilize the new capabilities of MSG.

Additional information on MSG is available on the EUMETSAT Web site at www.eumetsat.de (go to Meteosat Second Generation) and www.eumetsat.de/saf/.

ACKNOWLEDGMENTS. The paper has benefited from the contributions of many colleagues within EUMETSAT and from ESA. The authors thank them all for their contribution.

APPENDIX: LIST OF ACRONYMS

AGS	Applications ground segment
AMV	Atmospheric motion vectors
ATS	Applications Technology Satellite
ATSR	Along Track Scanning Radiometer
AVHRR	Advanced Very High Resolution Radiometer
CDS	Climate dataset
CLA	Cloud analysis product
CSR	Clear-Sky Radiance Product
CTH	Cloud-top height
ECMWF	European Centre for Medium-Range Weather Forecasts
EPS	EUMETSAT Polar System
ERS	Earth Remote Sensing Satellite
ESA	European Space Agency
EUMETSAT	European Organisation for the Exploitation of Meteorological Satellites
GERB	Geostationary Earth Radiation Budget instrument
GII	Global instability index
GOES	Geostationary Operational Environmental Satellite
GOME	Global Ozone Monitoring Experiment
GPS	Global positioning system

GRAS	GPS Receiver for Atmospheric Sounding
HIRS	High Resolution Infrared Sounder
HPI	High-resolution precipitation index
HRV	High-resolution visible channel
IDS	ISCCP dataset
IFOV	Instantaneous field of view
IMPF	Image Processing Facility
ISCCP	International Satellite Cloud Climatology Program
MPEF	Meteorological Product Extraction Facility
MSG	Meteosat Second Generation
MTH	Midtropospheric humidity product
MTSAT	Multi-functional Transport Satellite
NASA	National Aeronautics and Space Administration
NESDIS	National Environmental Satellite, Data, and Information Service
NIR	Near-infrared
NOAA	National Oceanic and Atmospheric Administration
NWP	Numerical weather prediction
RAL	Rutherford Appleton Laboratory
SAF	Satellite Application Facility
SEVIRI	Spinning Enhanced Visible and Infrared Imager
TH	Tropospheric humidity product
TOZ	Total ozone product
UK	United Kingdom
U-MARF	Unified Meteorological Archive and Retrieval Facility
UTH	Upper-tropospheric humidity product
VAS	VISSR Atmospheric Sounder
VISSR	Visible Infrared Spin-Scan Radiometer

REFERENCES

Arkin, P., and P. Xie, 1994: The Global Precipitation Climatology Project: First algorithm intercomparison project. *Bull. Amer. Meteor. Soc.,* **75**, 401–419.

Cihlar, J., A. Belward, and Y. Govaerts, 1999: Meteosat second generation opportunities for land surface applications. EUMETSAT–SAI Rep. EUM-SP-01, Joint Research Centre, Ispra, Italy, 67 pp.

Csekits, C., V. Zwatz-Meise, and A. Jam, 2000: Automatic detection of convective cells—A nowcast module at the Austrian Meteorological Service. *Proc. 2000 EUMETSAT Meteorological Satellite Data Users' Conf.,* Bologna, Italy, EUMETSAT EUM P 29, 715–721.

Dewitte, S., N. Clerbaux, L. Gonzalez, A. Hermans, A. Ipe, A. Joukoff, and G. Sadowski, 2000: Generation of GERB unfiltered radiances and fluxes. *Proc. 2000 EUMETSAT Meteorological Satellite Data Users' Conf.,* Bologna, Italy, EUMETSAT EUM P 29, 72–78.

Engelen, R., and S. Tjemkes, 2001: Ozone Retrievals from GOES sounder observations. *Proc. 2001 EUMETSAT Meteorological Satellite Data Users' Conf.,* Antalya, Turkey, EUMETSAT EUM P 33, 255–262.

Eyre, J., 2001: Planet Earth seen from space: Basic concepts. *Proc. Exploitation of the New Generation of Satellite Instruments for Numerical Weather Prediction.* Reading, United Kingdom, ECMWF, 5–19.

——, J. L. Brownscombe, and R. J. Allam, 1984: Detection of fog at night using Advanced Very High Resolution Radiometer (AVHRR) imagery. *Meteor. Mag.,* **113**, 266–271.

Govaerts, Y., A. Arriaga, and J. Schmetz, 2001: Operational vicarious calibration of the MSG/SEVIRI solar channels. *Adv. Space Res.,* **28,** 21–30.

Hamada, T., 1983: On the optimal time-interval of satellite image acquisition for operational cloud motion wind derivation. Meteorology Center of Japan Meteorological Agency Tech. Note 7, 79–87.

Harries, J. E., 2000: The geostationary Earth Radiation Budget Experiment: Status and science. *Proc. 2000 EUMETSAT Meteorological Satellite Data Users' Conf.,* Bologna, Italy, EUMETSAT EUM P-29, 62–71.

Holmlund, K., 1998: The utilization of statistical properties of satellite-derived atmospheric motion vectors to derive quality indicators. *Wea. Forecasting,* **13,** 1093–1104.

——, 2000: The Atmospheric Motion Vector retrieval scheme for Meteosat Second Generation. *Proc. Fifth Int. Winds Workshop,* Lorne, Australia, EUMETSAT EUM-P28, 201–208.

Inoue, T., 1987: A cloud type classification with *NOAA-7* split-window measurements. *J. Geophys. Res.,* **92** (D4), 3991–4000.

König, M., S. Tjemkes and J. Kerkmann, 2001: Atmospheric instability parameters derived from MSG SEVIRI observations. Preprints, *11th Conf. on Satellite Meteorology and Oceanography,* Madison, WI, Amer. Meteor. Soc., 336–338.

Lee, T. F., F. J. Turk, and K. Richardson, 1997: Stratus and fog products using *GOES-8–9* 3.9-μm data. *Wea. Forecasting,* **12**, 664–677.

Levizzani, V., P. Bougeault, H. Volkert, H. Mannstein, T. Kriebel, D. Frühwald, R. Benoit, and L. Garand, 1998: METEOSAT rapid scan during MAP-SOP. *MAP Newsletter,* No. 8, 17–19. [Available online at http://www.map.ethz.ch/NL8/METEOSAT.htm.]

——, J. Schmetz, H. J. Lutz, J. Kerkmann, P. P. Alberoni, and M. Cervino, 2001: Precipitation estimation from geostationary orbit and prospects for Meteosat Second Generation (MSG). *Meteor. Appl.,* **8**, 23–41.

Lindzen, R. S., M.-D. Chou, and A. Y. Hou, 2001: Does the earth have an adaptive infrared iris. *Bull. Amer. Meteor. Soc.,* **82,** 417–432.

Lutz, H. J., 1999: Cloud processing for Meteosat Second Generation. EUMETSAT Tech. Department Tech. Memo. 4, 26 pp.

Ma, X. L., T. Schmit, and W. L. Smith, 1999: A nonlinear physical retrieval algorithm—Its application to the *GOES-8/9* sounder. *J. Appl. Meteor.,* **38,** 501–513.

Menzel, W. P., and J. F. W. Purdom, 1994: Introducing GOES-I: The first of a new generation of Geostationary Operational Environmental Satellites. *Bull. Amer. Meteor. Soc.,* **75,** 757–781.

——, W. L. Smith, and T. R. Stewart, 1983: Improved cloud motion wind vector and altitude assignment using VAS. *J. Climate Appl. Meteor.,* **22,** 377–384.

——, F. C. Holt, T. J. Schmit, R. M. Aune, A. J. Schreiner, G. S. Wade, and D. G. Gray, 1998: Application of *GOES-8/9* soundings to weather forecasting and nowcasting. *Bull. Amer. Meteor. Soc.,* **79,** 2059–2077.

Munro, R., G. Kelly, M. Rohn, and R. Saunders, 1998: Assimilation of Meteosat radiance data within the 4DVAR system at ECMWF. *Proc. Fourth Int. Winds Workshop,* Saanenmöser, Switzerland, EUMETSAT EUM P-24, 299–306.

Nieman, S., J. Shmetz, and W. P. Menzel, 1993: A comparison of several techniques to assign heights to cloud tracers. *J. Appl. Meteor.,* **32,** 1559–1568.

Orsolini, Y. J., and F. Karcher, 2000: Total-ozone imaging over North America with *GOES-8* infrared measurements. *Quart. J. Roy. Meteor. Soc.,* **126,** 1557–1561.

Pinty, B., F. Roveda, M. M. Verstraete, N. Gobron, Y. Govaerts, J. V. Martonchik, D. J. Diner, and R. A. Kahn, 2000a: Surface albedo retrieval from Meteosat. Part 1: Theory. *J. Geophys. Res.,* **105,** 18 099–18 112.

——, ——, ——, ——, ——, ——, ——, and ——, 2000b: Surface albedo retrieval from Meteosat. Part 2: Applications. *J. Geophys. Res.,* **105,** 18 113–18 134.

——, M. M. Verstraete, N. Gobron, F. Roveda, Y. Govaerts, 2000c: Do human-induced fires affect the Earth surface reflectance at continental scale? *Eos, Trans. Amer. Geophys. Union,* **81,** 381–389.

Prata, A. J., 1989: Observations of volcanic ash clouds in the 10–12 μm window using AVHRR/2 data. *Int. J. Remote Sens.,* **10,** 751–761.

Prins, E., J. Schmetz, L. Flynn, D. Hillger, and J. Feltz, 2001: Overview of current and future diurnal active fire monitoring using a suite of international geostationary satellites. *Global and Regional Wildfire Monitoring: Current Status and Future Plans,* F. J. Ahern, J. G. Goldhammer, and C. O. Justice, Eds., SPB Academic Publishing, 145–170.

Purdom, J., 1996: Detailed cloud motions from satellite imagery taken at thirty second and three minute intervals. *Proc. Third Int. Winds Workshop,* Ascona, Switzerland, EUMETSAT EUM P-1, 137–145.

Riishojgaard, L. P., 1996: On four-dimensional variational assimilation of ozone data in weather prediction models. *Quart. J. Roy. Meteor. Soc.,* **122,** 1545–1571.

Rodgers, C., 2000: *Inverse Methods for Atmospheric Sounding: Theory and Practice.* Series on Atmospheric, Oceanic, and Planetary Physics, Vol. 2, World Scientific, 256 pp.

Rosci, P., A. Balzamo, L. De Leonibus, and F. Zauli, 2000: Improvements of automatic detection and extrapolation of convective phenomena using MAP rapid scan Meteosat images. *Proc. 2000 EUMETSAT Meteorological Satellite Data Users' Conf.,* Bologna, Italy, EUMETSAT EUM P-29, 797–804.

Rosenfeld, D., and I. W. Lensky, 1998: Satellite-based insights into precipitation formation processes in continental and maritime clouds. *Bull. Amer. Meteor. Soc.,* **79,** 2457–2476.

Rossow, W. B., and R. A. Schiffer, 1999: Advances in understanding clouds from ISCCP. *Bull. Amer. Meteor. Soc.,* **80,** 2261–2287.

Saunders, R. W., and K. T. Kriebel, 1988: An improved method for detecting clear sky and cloudy radiances from AVHRR data. *Int. J. Remote Sens.,* **9,** 123–150.

Schmetz, J., M. Mhita, and L. van de Berg, 1990: Meteosat observations of longwave cloud-radiative forcing for April 1985. *J. Climate,* **3,** 784–791.

——, K. Holmlund, J. Hoffman, B. Strauss, B. Mason, V. Gaertner, A. Koch, and L. van de Berg, 1993: Operational cloud motion winds from Meteosat infrared images. *J. Appl. Meteor.,* **32,** 1206–1225.

——, C. Geijo, W. P. Menzel, K. Strabala, L. van de Berg, K. Holmlund, and S. Tjemkes, 1995: Satellite observations of upper tropospheric relative humidity, clouds and wind field divergence. *Beitr. Phys. Atmos.,* **68,** 345–357.

Shenk, W. E., 1991: Suggestions for improving the derivation of winds from geosynchronous satellites. *Global Planet. Change,* **4,** 165–171.

Soden, B., and F. P. Bretherton, 1993: Upper tropospheric relative humidity from GOES 6.7 μm channel: Method and climatology for July 1987. *J. Geophys. Res.,* **98,** 16 669–16 688.

Szantai, A., F. Desalmand, M. Desbois, and P. Lecomte, 2000: Tracking low-level clouds over Central Africa

on Meteosat images. *Proc. 2000 EUMETSAT Meteorological Satellite Data Users' Conf.,* Bologna, Italy, EUMETSAT EUM P-29, 813–820.

Tjemkes, S. A., and J. Schmetz, 1997: Synthetic satellite radiances using the radiance sampling method. *J. Geophys. Res.,* **102** (D2), 1807–1818.

——, and P. Watts, 2000: Cloud properties from Meteosat. *Proc. 2000 EUMETSAT Meteor. Satellite Data Users' Conf.,* Bologna, Italy, EUMETSAT EUM-P29, 314–317.

Uchida, H., T. Oshima, T. Hamada, and S. Osano, 1991: Low-level cloud motion wind field estimated from GMS short interval images in typhoon vicinity. *Geophys. Mag.,* **44,** 37–50.

Velden, C., D. Stettner, and J. Daniels, 2000: Wind vector fields derived from GOES rapid-scan imagery. Proc. 10th Conf. on Satellite Meteor. and Oceanogr., Long Beach California, Amer. Meteor. Soc., 20–23.

Watkin, S., M. Ringer, and A. Baran, 2000: Investigation into the use of SEVIRI imagery for the automatic detection of volcanic ash clouds. *Proc. 2000 EUMETSAT Meteor. Satellite Data Users' Conf.,* Bologna, Italy, EUMETSAT EUM P-29, 753–760.

Wiegner, M., P. Seifert, and P. Schlüssel, 1998: Radiative effect of cirrus clouds in Meteosat Second Generation spinning enhanced visible and infrared imaging channels. *J. Geophys. Res.,* **103** (D18), 23 217–23 230.